A Systematic and Efficient Approach for Data Association in Topological Maps for Mobile Robot using Wavelet Transformation

N.L.Doh, K.Lee, and W.K.Chung

Department of Mechanical Engineering, POSTECH, San 31, Pohang, Korea
(Tel: +82-54-279-2844; Fax: +82-54-279-8459; Email:{nakji,lekomin,wkchung}@postech.ac.kr)

Abstract: Data association is a process that matches a recent observation with known data set, which is used for the localization of mobile robots. Edges in topological maps have rich information which can be used for the data association. However, no systematic approach on using the edge data for data association has been reported. This paper proposes a systematic way of utilizing the edge data for data association. First, we explain a Local Generalized Voronoi Angle(LGA) to represent the edge data in 1-dimension. Second, we suggest a key factor extraction procedure from the LGA to reduce the number by 2^7-2^8 times, for computational efficiency using the wavelet transformation. Finally we propose a way of data association using the key factors of the LGA. Simulations show that the proposed data association algorithm yields higher probability for similar edges in computationally efficient manner.

Keywords: Localization, Topological Map, Generalized Voronoi Graph, Data Association.

1. Introduction

Topological maps are consist of nodes and edges. The nodes are topologically meaningful places such as junctions, doors, etc, and the edges are connections between nodes. The node has been used for various data association algorithms [1–4] which match a recent observation with known data set for the localization of mobile robots.

However, little attention has been given on using the edge data for the data association [5, 6], even though it has rich information such as length, shape, effects of obstacles and so on. Moreover, if cheap sensors(such as ultrasonic sensors) are used, the edge has an advantage over the node because of the large number of sensor readings. In the node, only a few recent sensor readings, which are stained by sensor noises, are contained. In the edge, however, a large number of accumulated data, whose noises could be removed by various algorithms [7, 8], is included.

In this paper, a systematic and efficient way for the data association especially for the edge is proposed. First, a Local Generalized Voronoi graph Angle(LGA in short) is explained as the most representative data in the edge. Recall that the Generalized Voronoi Graph(GVG in short) is a topological representation, which consists of a set of points that are equidistant to two or more objects(*i.e.* the medial line). Thus the angle of the GVG can represent the detailed shape of the edge. By using the LGA, large portions of the edge data such as effects of obstacles, irregularity and overall shape of the edge can be expressed in 1-dimension.

Even though the LGA is 1-dimensional, it consists of large number of samples. For example, a LGA of an edge (whose length and control frequency are 10m, 10Hz with $0.1m/sec$ velocity) has 1000 samples. If a data association algorithm such as [9] tries to compare a recent LGA observation with large numbers of known LGAs, it will suffer from computational burden.

This research was supported by the National Research Laboratory (NRL) Program (M1-0302-00-0040-03-J00-00-024-00) of the Ministry of Science & Technology, Republic of Korea.

To reduce the number of samples of the LGA, we developed an efficient way that uses a key factor. The key factor is a set of meaningful information in the LGA, and its number is smaller than the LGA by 2^7-2^8 times. We adopted the wavelet transformation [10], which divides the LGA into its various frequencies, for key factor extraction.

Finally, a data association algorithm which uses the key factor of the LGA is suggested. This algorithm is computationally efficient because it uses the key factor, and simulation results show that the proposed data association algorithm yields higher probability for similar edges.

This paper is organized as follows. In section 2, the local GVG angle(LGA) is illustrated. The extraction of key factors from the LGA is suggested with a brief introduction of the wavelet transformation in section 3. Section 4explains a data association scheme using the key factors. In section 5. , simulation results are given which validate the efficiency of the proposed data association, and conclusion follows.

2. Local generalized Voronoi diagram angle

There are abundant data in the edge such as length, shape, irregularities, width of edges, etc. For the efficient representation, however, the most representative data should be selected among them.

One possible candidate is the edge of the generalized Voronoi graph(GVG in short) [1]. Recall that the GVG is a set of points whose edges and nodes are equidistant to two or more obstacles. Fig. 1 shows a connection of edges of the GVG(denoted by $E_{\alpha,\beta}$) from node $\alpha(N_\alpha)$ to node $\beta(N_\beta)$.

In $E_{\alpha,\beta}$, three meaningful data are included as follows:

- the effects of obstacles in the region A, B(Fig. 1).
- the irregularity of the edge in the region C(Fig. 1).
- the overall shape of the edge.

The $E_{\alpha,\beta}$ is a discrete set of position and heading angle of a robot which had traced the GVG. Among these, the heading angle contains three fore-mentioned data. Thus we select the heading angle as the most representative data of the GVG edge.

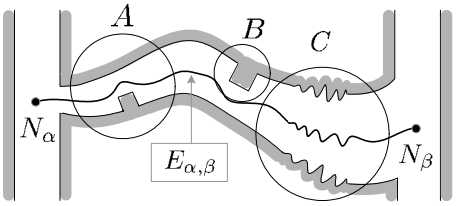

Fig. 1. A connection of edges of the GVG denoted by $E_{\alpha,\beta}$.

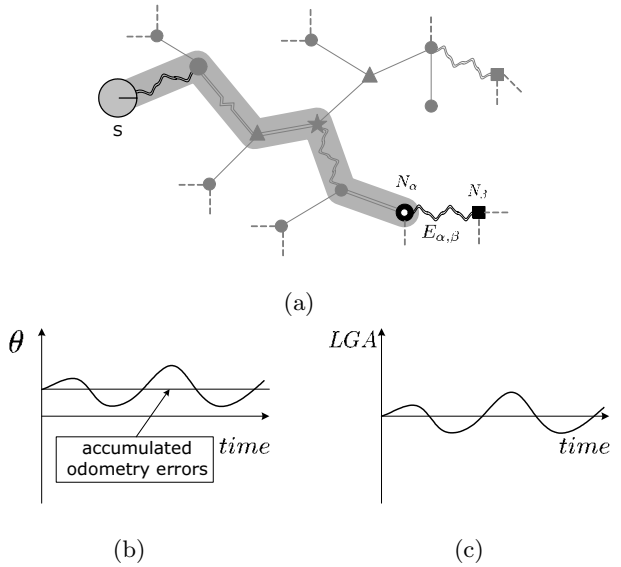

Fig. 2. An illustration of the local GVG angle(LGA): (a) A robot had navigated from S to node N_β through the shaded path. (b) The angle of $E_{\alpha,\beta}$(denoted by θ) is affected by accumulated odometry errors, but (c) the LGA is not.

However, the heading angle is affected by accumulated odometry errors as shown in Fig. 2(a,b). So we suggest *an Local GVG Angle*(LGA in short) where the *'local'* denotes that the origin of the LGA lies on the start node as shown in Fig. 2(c).

3. Extraction of key factors from the LGA

The LGA is designed for the data association which matches a recent LGA observation with one of known LGAs. One critical problem in the data association of the LGA is computational burden. For example, let us consider the following case. A topological map consists of 200 edges, and each edge had been represented by the LGA. The number of samples in each LGA is around 1000(10Hz control frequency and 10m edge length with $0.1m/sec$ velocity). If a data association algorithm in [9] is used[1], the recent LGA should be compared by 200×3^5 times. Then the total calculation is 4.86×10^7 which is intractable in real time.

A possible solution is to reduce the sample number of each LGA by extracting key factors, whose number is smaller than the LGA by 2^7-2^8 times. By using the key factors, the computation of the previous example is reduced into 3.8×10^5 - 1.9×10^5.

The key factors can be extracted by using the wavelet transformation [10] which divides the LGA into its various frequencies.

[1] for the depth of inspection: 5, the number of edges for each node: 3.

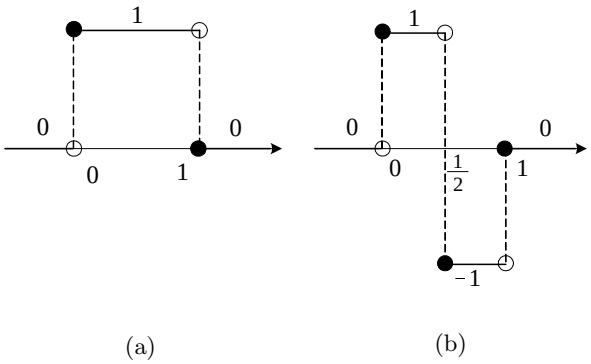

Fig. 3. Graphs of (a) the Haar scaling function $\phi(x)$ and (b) the Haar wavelet $\psi(x)$.

3.1. Wavelet transformation

This subsection briefly explains the wavelet transformation by referring [10].

Definition 1: *The Haar scaling function is defined as*

$$\phi(x) = \begin{cases} 1, & \text{if} \quad 0 \le x < 1 \\ 0, & \text{elsewhere.} \end{cases}$$

The graph of the Haar scaling function is given in Fig. 3(a).

Definition 2: *Suppose j is any nonnegative integer. The space of step functions at level j, denoted by V_j is defined to be the space spanned by the set*

$$\{\cdots, \phi(2^j x + 1), \phi(2^j), \phi(2^j x - 1), \phi(2^j x - 2), \cdots\}$$

over the real numbers. V_j is the space of piecewise constant functions of finite support whose discontinuities are contained in the set

$$\{\cdots, -1/2^j, 0, 1/2^j, 2/2^j, 3/2^j, \cdots\}.$$

Definition 3: *The Haar wavelet is the function*

$$\psi(x) = \phi(2x) - \phi(2x - 1).$$

Its graph is given in Fig. 3(b).

Then following theorems holds.

Theorem 1: *Let W_j be the space of functions of the form*

$$\sum_{k \in Z} a_k \psi(2^j x - k) \qquad a_k \in R$$

where we assume that only a finite number of a_k are nonzero. W_j is the orthogonal complement of V_j in V_{j+1} and

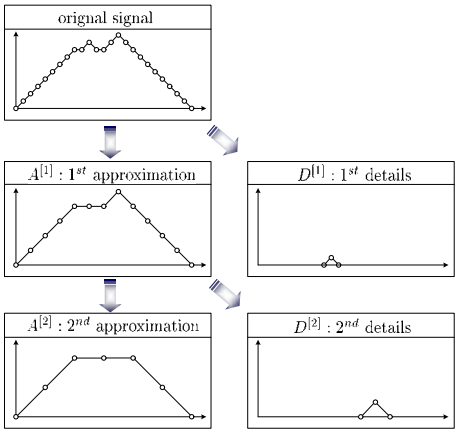

Fig. 4. An original signal is decomposed into $A^{[1]}$ and $D^{[1]}$,and $A^{[1]}$ is divided into $A^{[2]}$ and $D^{[2]}$.

$$V_{j+1} = V_j \oplus W_j$$

where $A \oplus B$ denotes that A and B are orthogonal to each other.

Theorem 2: *Suppose*

$$f_j(x) = \sum_{k \in Z} a_k^j \phi(2^j x - k) \in V_j.$$

Then f_j can be decomposed as

$$f_j = w_{j-1} + f_{j-1}$$

where

$$\begin{aligned} w_{j-1} &= \sum_{k \in Z} b_k^{j-1} \psi(2^{j-1} x - k) \in W_{j-1} \\ f_{j-1} &= \sum_{k \in Z} a_k^{j-1} \phi(2^{j-1} x - k) \in V_{j-1} \end{aligned}$$

with

$$b_k^{j-1} = \frac{a_{2k}^j - a_{2k+1}^j}{2}, \quad a_k^{j-1} = \frac{a_{2k}^j + a_{2k+1}^j}{2}.$$

Theorem 1, 2 explain that an original signal f_j can be decomposed as

$$f_j = w_{j-1} + w_{j-2} + \cdots + w_0 + f_0. \tag{1}$$

To make it clear, let us define an approximation and a detail of f_i as

$$\begin{aligned} A^{[i]} &= f_{j-i} \\ D^{[i]} &= w_{j-i} \end{aligned} \tag{2}$$

Here $A^{[*]}$ reveals the overall shape of the original signal, and $D^{[*]}$ shows the time and magnitude of the frequency of level $[*]$. The physical meaning of the wavelet transformation is that an original signal can be decomposed into the approximation and the detail of one lower level as shown in Fig. 4.

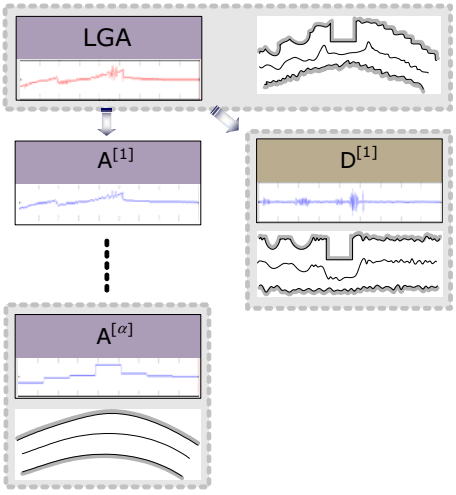

Fig. 5. The LGA can be decomposed into its various frequencies by the wavelet transform. The LGA contains the effects of obstacles, irregularity and overall shape. Among these, the effects of obstacle and the irregularity is expressed by the $D^{[1]}$, and the overall shape is revealed by $A^{[\alpha]}$ where α is close to the final level of decomposition.

3.2. Key factor extraction

Three characteristics of the edge are included in the LGA. These are the effects of obstacles, the irregularity and the overall shape of the GVG edge. Among these, the effects of obstacles and the irregularity of the edge are reflected in rapid changes of the LGA. Thus these two characteristics correspond to the high frequency component of the LGA. In contrast, the overall shape of the edge falls into the low frequency part of the LGA.

In the wavelet transformation, the high frequency component is reflected in the $D^{[1]}$(Fig. 5), and the low frequency part is contained in $A^{[\alpha]}$(Fig. 5) where α is close to the final level of the decomposition.

Thus we define local key factors from $D^{[1]}$ to represent the effects of obstacles and the irregularity of the edge. Also we extract global key factors from $A^{[\alpha]}$ to express the overall shape of the edge.

3.2.1 Local key factor extraction

Let us denote the following terms for the local key factor extraction.

- μ: the number of samples in a LGA.
- $c(\mu, k) = \ulcorner \frac{\mu}{2^k} \urcorner$ where $\ulcorner(\cdot)\urcorner$ denotes the least integer greater than or equal to $(\cdot)$.
- $\underset{i}{A}$: the $i-th$ element of the set A.
- $\#(A)$: the number of samples in the set A.

The local key factor can be extracted as in the following. Define a set of squares of $D^{[1]}$ as

$$V = \{\underset{1}{V}, \underset{2}{V}, \cdots, \underset{c(\mu,1)}{V}\}, \tag{3}$$

where $\underset{i}{V} = (\underset{i}{D^{[1]}})^2$.

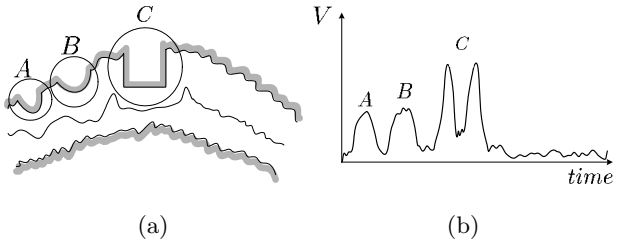

(a) (b)

Fig. 6. Figure of (a) an Edge and (b) its plot of V.

For example, Fig. 6(a,b) show an edge and a plot of V where the effects of obstacles and the irregularity of the edge is contained. In Fig. 6, two half-circle obstacles in the region A, B are reflected as two middle peaks, and one rectangular obstacle in the region C is shown as two high peaks in the center. The irregularity also expressed as small fluctuations throughout all times.

Thus by dividing V according to its magnitude, the effects of obstacles and the irregularity can be identified.

For the division, let us fix a reference value as ${}_{max}v$ which is the maximum angular acceleration of a robot. Also, define *a Depth of Local inspection*(DL in short) to specify the number of the division. Now define

$$\Gamma^{[l]} = \{(\gamma_1^{[l]}, t_1^{[l]}), (\gamma_2^{[l]}, t_2^{[l]}), \cdots, (\gamma_{\#(\Gamma^{[l]})}^{[l]}, t_{\#(\Gamma^{[l]})}^{[l]})\}, \qquad (4)$$

where

$$\gamma_i^{[l]} = \text{ the } i-th \text{ signals among } \underset{(\cdot)}{V} \text{ that satisfies}$$
$$\begin{cases} (\frac{1}{2})^l {}_{max}v < \underset{(\cdot)}{V} \leq (\frac{1}{2})^{l-1} {}_{max}v & \text{if } l \neq DL, \\ 0 < \underset{(\cdot)}{V} \leq (\frac{1}{2})^{DL-1} {}_{max}v & \text{if } l = DL. \end{cases}$$

Here $t_i^{[l]}$ is the time that $\gamma_i^{[l]}$ occurred. Fig. 7(b-d) are examples of $\Gamma^{[1]}, \Gamma^{[2]}, \Gamma^{[3]}$ for $DL = 3$. In Fig. 7(b), one can observe an existence of big obstacle. The effects of two small obstacles are shown in Fig. 7(c), and the irregularity is revealed in Fig. 7(d).

Now, the local key factors are defined as

$$\Lambda^{[l]} = \sum_{i=1}^{\#(\Gamma^{[l]})} \gamma_i^{[l]}, \qquad (5)$$

$$\Sigma^{[l]} = \left[\frac{1}{\#(\Gamma^{[l]})} \sum_{i=1}^{\#(\Gamma^{[l]})} \left\{ t_i^{[l]} - \overline{t_i^{[l]}} \right\}^2 \right]^{\frac{1}{2}}, \qquad (6)$$

where $\overline{t_i^{[l]}}$ is the average of $t_{(\cdot)}^{[l]}$.

Here $\Lambda^{[l]}$ expresses the effects of obstacles and the irregularity of the edge, and $\Sigma^{[l]}$ represent the standard deviation of the location of the obstacles.

3.2.2 Global key factor extraction

The global key factors can be simply defined as in the following. Let us define *a Depth of Global inspection*(DG in short) Then the approximation at level $DG(A^{[DG]})$ is selected as the global key factors. The DG should be selected so that $A^{[DG]}$ is capable of representing the overall shape of the LGA.

Our suggestion for the DG is 7-8 which approximates the LGA by using $c(\mu, 7)$-$c(\mu, 8)$ data ($i.e.$ $\ulcorner \frac{\mu}{2^7} \urcorner$-$\ulcorner \frac{\mu}{2^8} \urcorner$).

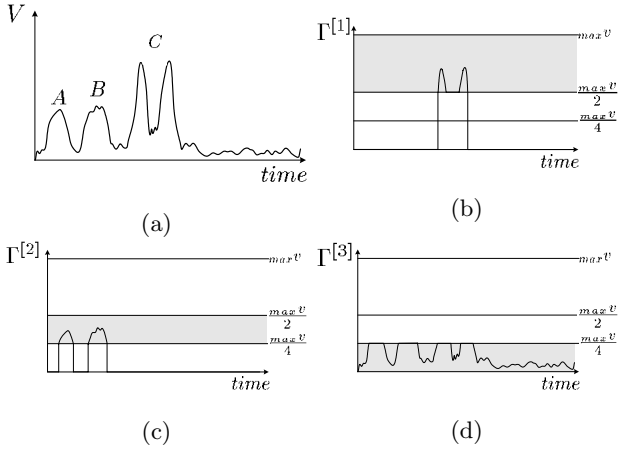

(a) (b) (c) (d)

Fig. 7. Γ values of (a) the V. (b-d) are $\Gamma^{[1]}$, $\Gamma^{[2]}$ and $\Gamma^{[3]}$. In (b), one can observe an existence of big obstacle. The effects of two small obstacles are shown in (c), and the irregularity is revealed in (d).

3.2.3 Remarks on the key factors

The total number of the local key factors is $2 \times DL$, and that of the global key factors is $c(\mu, DG) = \ulcorner \frac{\mu}{2^{DG}} \urcorner$. Thus the number of the LGA is approximately reduced by 2^{DG} times because $2 \times DL << \mu$.

One important question is whether these key factors effectively reflect the characteristics of edges. This question will be validated by a data association scheme and simulation results in the following chapters.

4. Data association scheme

This section provides a data association scheme for the edges, which uses the key factors in the section 3. Let us assume that a reference edge ${}^{ref}E$ and a candidate edge ${}^{can}E$ is given. From here on, the ref, can in the upper-left corner denote the reference and the candidate.

For local key factor comparison, we define a one-to-one comparison

$$\begin{aligned} \Delta\Lambda(ref, can) &= \sum_{i=1}^{DL} |{}^{ref}\Lambda^{[i]} - {}^{can}\Lambda^{[i]}|, \\ \Delta\Sigma(ref, can) &= \sum_{i=1}^{DL} |{}^{ref}\Sigma^{[i]} - {}^{can}\Sigma^{[i]}|, \end{aligned} \qquad (7)$$

to represent the differences of the power and standard deviation of two edge's $\Lambda^{[\cdot]}, \Sigma^{[\cdot]}$.

In the global key factors, however, the one-to-one comparison is unavailable, because the number of ${}^{ref}A^{[DG]}$ is not always the same with that of ${}^{can}A^{[DG]}$. For the comparison, we first define an algorithm called **LCMcompare** which extends the

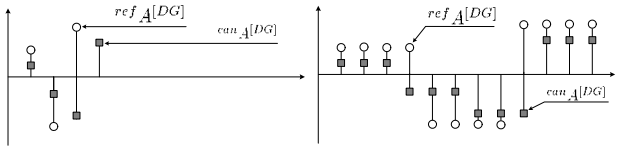

(a) (b)

Fig. 8. An example of the data number extension using the least common multiple. In (a), the one-to-one comparison is unavailable . However, after the extension, the one-to-one comparison can be performed.

number of the $^{ref}A^{[DG]}$ and $^{can}A^{[DG]}$ to their least common multiple as follows:

Algoritm LCMcompare(E_a, E_b)

c $\leftarrow$ least common multiple of $\#(E_a), \#(E_b)$.

$$E_a(ext) = \{\underset{1}{E_a(ext)} = \cdots = \underset{c/\#(E_a)}{E_a(ext)} = \underset{1}{E_a}, \cdots, \underset{c-\#(E_a)/c+1}{E_a(ext)} = \cdots = \underset{c}{E_a(ext)} = \underset{\#(E_a)}{E_a}\}$$

$$E_b(ext) = \{\underset{1}{E_b(ext)} = \cdots = \underset{c/\#(E_b)}{E_b(ext)} = \underset{1}{E_b}, \cdots, \underset{c-\#(E_b)/c+1}{E_b(ext)} = \cdots = \underset{c}{E_b(ext)} = \underset{\#(E_b)}{E_b}\}$$

return $\frac{1}{c}\sum_{i=1}^{c} |\underset{i}{E_a(ext)} - \underset{i}{E_b(ext)}|$

Fig. 8 shows an example of the data extension in the **LCMcompare**. Here $^{ref}A^{[DG]}$ consists of 3 samples, and $^{can}A^{[DG]}$ has 4 samples. The least common multiple is 12. Then $^{ref}A^{[DG]}$ is extended by 4(12/3) times, and $^{can}A^{[DG]}$ by 3(12/4) times for the one-to-one comparison.
Now, global key factor comparison is given as

$$\Delta A^{DG}(ref, can) = LCMcompare(^{ref}A^{DG}, ^{can}A^{DG}). \quad (8)$$

Till now, three measures, $\Delta\Lambda, \Delta\Sigma, \Delta A^{[DG]}$, are defined for a candidate edge. For many candidate edges, these measures should be normalized for even comparison. For that purpose, define a normalizer

$$\aleph\left(\underset{i}{f}\right) = \frac{1}{\#(f)} \frac{\underset{i}{f}}{\sum_{j=1}^{\#(f)} \underset{j}{f}}, \quad (9)$$

for a set of functions f.
Finally, let us define *a probability density function*(pdf in short) of ^{can}E to be ^{ref}E as

$$P(^{can}E = ^{ref}E) = \aleph(\aleph(\Delta\Lambda) \times \aleph(\Delta\Sigma) \times \aleph(\Delta A^{[DG]})). \quad (10)$$

Then, a data association of edges can be performed by selecting pdfs whose values are larger than a certain threshold. The threshold can be chosen as a multiple of a marginal value. The marginal value is $\frac{1}{\eta}$ where η is the numbers of the candidates. Here $P(^{can}E = ^{ref}E) = \frac{1}{\eta}$ means that no information can be provided for the candidate. If $P(^{can}E = ^{ref}E) > \frac{1}{\eta}$, the candidate is likely to be the reference edge and vice versa.

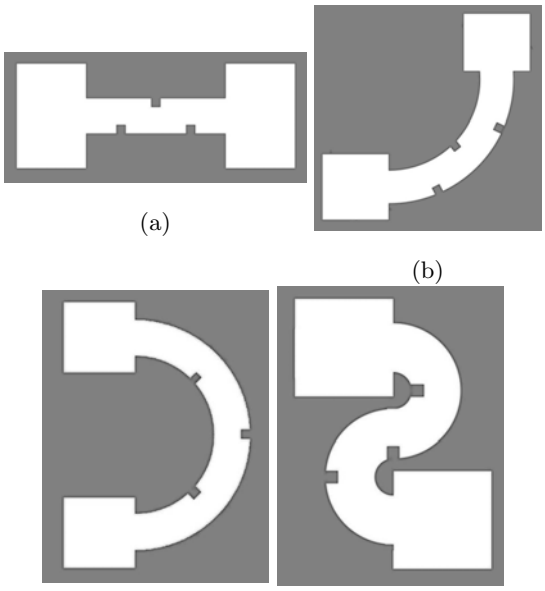

(a) (b) (c) (d)

Fig. 9. The reference and candidate edges that are used for the first simulations. (a) is used as the reference and the first candidate edge. (b-d) are examples of the other 38 candidate edges whose shapes are different from the reference edge.

5. Simulation results

This section provides simulations to prove that the key factors effectively reveals the characteristics of the LGA. The simulations are preformed for a robot with 36 distant sensors. A Gaussian error, $\mathcal{N}(\prime, \sigma^{\in})$, whose 2σ corresponds to 20% of the odometry and the distance, is added to the real odometry and the real distance.
The first simulation is performed as follows:
1. Get key factors from a reference edge(Fig. 9(a)).
2. Get key factors from a set of candidate edges which consists of the reference edge and 39 edges with different shapes(Fig. 9).
3. Calculate the pdf in Eq.(10) for all candidate edges.
4. Select edges whose pdf is larger than a certain threshold as a data-associated edge.

Fig. 10 shows the simulation result. The thin line shows the threshold(2/40) whose value is double of the marginal value. In this figure, only the pdf of the reference edge(1) is higher than the threshold, and the total sum of other 39 edges is close to the marginal value.
The second simulation is conducted for candidate edges which consist of a reference edge, a very similar edge with the reference and a set of 18 similar edges as shown in Fig. 11. The result is shown in Fig. 12, where the pdfs of the reference edge(1,Fig. 11(a)) and the very similar edge(2,Fig. 11(b)) are higher than the threshold(2/20). Suppose that the upper obstacle in Fig. 12(a) is a door, and the door is temporarily

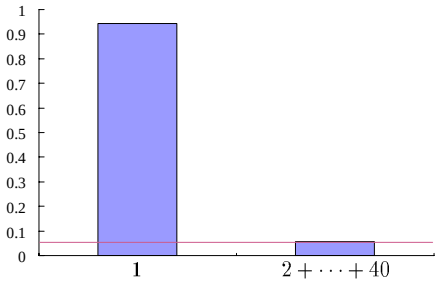

Fig. 10. The probability density functions of the first simulation.

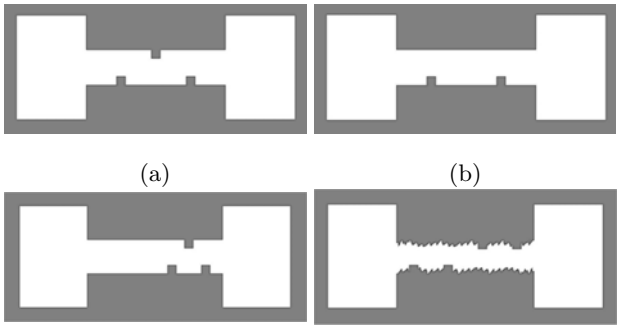

Fig. 11. The reference and candidate edges that are used for the second simulations. (a) is used as the reference and the first candidate edge. (b) the second candidate edge which is a very similar with the reference edge. (c,d) are examples of the other 18 similar edges.

closed in Fig. 12(b), then the proposed algorithm will give the highest probability to Fig. 12(b) among other candidates. This means that the algorithm can be extended to dynamic environment cases and this should be further investigated. These two simulations validate that the key factors reflect the meaningful data of the LGA in small numbers.

6. Conclusion

This paper proposed an systematic and efficient way of utilizing the edge data for the data association.

First, we explained a Local Generalized Voronoi Angle(LGA) to represent the edge data in 1-dimension. The LGA reflects effects of obstacles, irregularity and overall shape of edges.

Second, we suggested a key factor extraction procedure from the LGA to reduce the number for computational efficiency. The key factors consist of local key factor and global key factor. The local key factor represents the effects of obstacles and the irregularity of edges. The global key factor reveals the overall shape of edges. The total number of key factors are lower than the LGA by 2^7-2^8 times.

Finally we proposed a way of data association using the key factors of the LGA. This data association algorithm is computationally efficient because it uses the key factors.

Simulation results validated that the proposed data association algorithm yields higher probability for similar edges in computationally efficient manner.

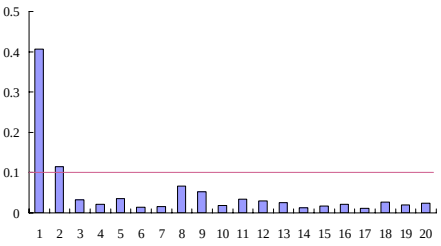

Fig. 12. The probability density functions of the second simulation.

References

[1] H. Choset and K. Nagatani, "Topological SLAM: Toward exact localization without explicit localization," *IEEE Trans. on Robotics and Automation*, pp. 125–137, 2001.

[2] M. Piaggio, A. Sgorbissa, and R. Zaccaria, "Global localisation via sub-graph isomorphism," in *European Workshop on Advanced Mobile Robots*, pp. 151–158, 1999.

[3] N. Tomatis, I. Nourbakhsh, and R. Siegwart, "Hybrid simultaneous localization and map building: Closing the loop with multiple-hypotheses tracking," in *International Conference on Robotics and Automation*, pp. 2749–2754, 2002.

[4] T. Bailey, E. M. Nebot, J. K. Rosenblatt, and H. F. Durrant-Whyte, "Data association for mobile robot navigation: A graph theoretic approach," in *International Conference on Robotics and Automation*, pp. 2512–2517, 2000.

[5] K. Nagatani and H. Choset, "Toward robust sensor based exploration by constructing reduced generalized Voronoi graph," in *Proc. of IEEE/RSJ Int. Conf. on Intelligent Robots and Systems*, pp. 1687–1692, 1999.

[6] M. Kruusmaa, "Global navigation in dynamic environments using case-based reasoning," *Autonomous Robots*, no. 14, pp. 71–91, 2003.

[7] H. Choset, K. Nagatani, and N. A. Lazar, "The arc-transversal median algorithm: A geometric approach to increasing ultrasonic sensor azimuth accuracy," *IEEE Trans. on Robotics and Automation*, vol. 19, no. 3, pp. 513–523, 2003.

[8] R. Grabowski, P. Khosla, and H. Choset, "An enhanced occupancy map for exploration via pose separation," in *International Conference on Robotics and Automation*, pp. 1691–1696, 2003.

[9] N. L. Doh, K. Lee, and W. K. Chung, "A localization algorithm using cheap sensors in topological maps with dynamic uncertainty," in *Proc. of IEEE/RSJ Int. Conf. on Intelligent Robots and Systems*, 2004. submitted and available at http://rnb.postech.ac.kr.

[10] A. Boggess and F. J. Narcowich, *A First Course in Wavelets with Fourier Analysis*. Prentice Hall, 2001.